

Privacy Enhanced PEFT: Tensor Train Decomposition Improves Privacy Utility Tradeoffs under DP-SGD

Pradip Kunwar

Tennessee Tech University,
Los Alamos National Laboratory
Cookeville, Tennessee, USA
pkunwar42@tnstate.edu

Maanak Gupta

Tennessee Tech University
Cookeville, Tennessee, USA
mgupta@tnstate.edu

Minh N. Vu

Los Alamos National Laboratory
Los Alamos, New Mexico, USA
mvu@lanl.gov

Manish Bhattacharai

Los Alamos National Laboratory
Los Alamos, New Mexico, USA
ceodsp@lanl.gov

Abstract

Fine-tuning large language models on sensitive data poses significant privacy risks, as membership inference attacks can reveal whether individual records were used during training. While Differential Privacy (DP) provides formal protection, applying DP to conventional Parameter-Efficient Fine-Tuning (PEFT) methods such as Low-Rank Adaptation (LoRA) often incurs substantial utility loss. In this work, we show that a *more structurally constrained* PEFT architecture, Tensor Train Low-Rank Adaptation (TTLoRA), can improve the privacy–utility tradeoff by shrinking the effective parameter space while preserving expressivity. To this end, we develop TTLoRA-DP, a differentially private training framework for TTLoRA. Specifically, we extend the ghost clipping algorithm to Tensor Train cores via cached contraction states, enabling efficient Differentially Private Stochastic Gradient Descent (DP-SGD) with exact per-example gradient norm computation without materializing full per-example gradients. Experiments on GPT-2 fine-tuning over the Enron and Penn Treebank datasets show that TTLoRA-DP consistently strengthens privacy protection relative to LoRA-DP while maintaining comparable or better downstream utility. Moreover, TTLoRA exhibits lower membership leakage even without DP training, using substantially smaller adapters and requiring on average 7.6× fewer parameters than LoRA. Overall, our results demonstrate that TTLoRA offers a practical path to improving the privacy–utility tradeoff in parameter-efficient language model adaptation.

CCS Concepts

- Security and privacy → Privacy protections; Privacy-preserving protocols.

Permission to make digital or hard copies of all or part of this work for personal or classroom use is granted without fee provided that copies are not made or distributed for profit or commercial advantage and that copies bear this notice and the full citation on the first page. Copyrights for components of this work owned by others than the author(s) must be honored. Abstracting with credit is permitted. To copy otherwise, or republish, to post on servers or to redistribute to lists, requires prior specific permission and/or a fee. Request permissions from permissions@acm.org.

CCS '26, The Hague, The Netherlands

© 2026 Copyright held by the owner/author(s). Publication rights licensed to ACM.
ACM ISBN 978-x-xxxx-xxxx-x/YYY/MM
https://doi.org/10.1145/nnnnnnnn.nnnnnnnn

Keywords

Differential Privacy, Privacy Utility Tradeoff, Tensor Train Decomposition, Parameter Efficient Fine Tuning (PEFT)

ACM Reference Format:

Pradip Kunwar, Minh N. Vu, Maanak Gupta, and Manish Bhattacharai. 2026. Privacy Enhanced PEFT: Tensor Train Decomposition Improves Privacy Utility Tradeoffs under DP-SGD. In *Proceedings of ACM Conference on Computer and Communications Security (CCS '26)*. ACM, New York, NY, USA, 15 pages. <https://doi.org/10.1145/nnnnnnnn.nnnnnnnn>

1 Introduction

The deployment of Large Language Models (LLMs) in privacy-sensitive settings—such as healthcare, finance, and legal services often requires fine-tuning on confidential corpora [5, 8]. While Full Fine-Tuning (FFT) achieves high utility, its massive parameter count poses significant challenge for computational efficiency [12, 13]. Parameter-Efficient Fine-Tuning (PEFT) methods, most notably LoRA, address the challenge by adapting only a small subset of parameters, significantly reducing memory and computation requirements [13]. However, LoRA’s two-factor matrix design imposes a fundamental *parameter floor*, restricting how lightweight the adapters can be without degrading performance. Tensor Train Low-Rank Adaptation (TTLoRA) [2], a structurally constrained PEFT that leverages Tensor Train (TT) decomposition [26, 27], overcomes this limitation. It organizes the adaptation into a 3rd-order chain of tensor cores, enabling an ultra-low-parameter regime that maintains expressivity and competitive task performance [15].

Beyond parameter efficiency, how PEFT architectures shape model privacy leakage remains underexplored. Fine-tuning on sensitive datasets raises risks of Membership Inference Attacks (MIA) [20, 30, 37]. While LoRA exhibits some inherent privacy benefits—due to implicit regularization and noise-like optimization dynamics [9, 23]—these effects are often insufficient, leaving models vulnerable [20, 28]. Differential Privacy (DP) can mitigate the leakage [22, 28], but applying DP to LoRA typically comes at a substantial utility cost [9, 31, 33]. This raises a key question: *Can a more structurally constrained PEFT method like TTLoRA yield stronger inherent privacy and more favorable DP utility trade-offs while operating in an ultra-low parameter regime?*

In this work, we show that TTLoRA empirically delivers a more favorable privacy–utility tradeoff than LoRA, both with and without

DP training. The tensor train structure enables adapters that are simultaneously smaller, expressive [15], and implicitly regularized [29], reducing sample-specific memorization. Building on this, we develop **TTLLoRA-DP**, the first Differentially Private Stochastic Gradient Descent (DP-SGD) pipeline for TTLLoRA, and demonstrate that it consistently improves empirical privacy (MIA robustness) and retains competitive utility under both DP and non-DP training.

We evaluate the impact of TTLLoRA's tensor train structure along two axes that are critical in practice: (i) **DP utility**—measuring task performance across different privacy budgets ϵ (smaller ϵ indicates stronger privacy), and (ii) **empirical leakage under DP**—tracking performance versus membership leakage MIA AUC (lower is better) across the same privacy budgets. We further investigate whether the observed effects persist **without DP**, measuring membership leakage against performance. To quantify leakage, we implement the state-of-the-art loss-based attack protocol PreCurious¹ [20]. For DP evaluation, we consider multiple privacy budgets, $\epsilon = \{0.5, 1, 3, 5\}$, using RDP accounting [25] with $\delta = 8 \times 10^{-6}$ or $N^{1.1}$ (where N = number of samples). Specifically, our contributions are as follows:

- **Higher Utility under Private Training:** TTLLoRA consistently achieves stronger utility under DP compared to LoRA across all ϵ budgets. For example, on the Enron dataset at a strict privacy budget of $\epsilon = 0.5$, TTLLoRA achieves an average perplexity of 27.52 (lower is better), outperforming LoRA's 29.29 (see Table 2).
- **Robustness against MIA Leakage under DP:** When tested under PreCurious attack protocol, TTLLoRA fundamentally alters how membership leakage scales with the privacy budget. On Enron, as ϵ increases, LoRA exhibits a significant rise in vulnerability, with average attack AUC (MIA leakage) increasing from 52.49% to 58.43%, whereas TTLLoRA remains nearly stable, changing only from 51.36% to 52.04% (see Fig. 1 and Table 3). Importantly, these privacy gains incur negligible utility loss, with perplexity differences consistently limited to 0.01.
- **Stronger Inherent Privacy Without DP:** Beyond DP, TTLoRA exhibits substantially lower membership leakage even without DP-SGD. On Enron, TTLLoRA reduces average attack AUC (MIA leakage) to 88.68% and FPR@1% to 16.19%, compared to 94.91% and 33.47% for LoRA, while maintaining comparable perplexity (18.05 vs. 17.46). Calibrated loss distributions (Fig. 2) show significantly greater overlap between member and non-member losses, indicating reduced sample-specific memorization due to the tensor train structure.

Taken together, these results indicate that privacy-preserving adaptation of LLMs need not rely solely on stronger DP mechanisms or tighter privacy budgets. Instead, the structured tensor train decomposition in TTLLoRA—which imposes a compositional constraint while reducing the effective parameter space—significantly shapes both utility and privacy leakage. By operating well below the practical parameter floor of conventional LoRA, TTLLoRA enables effective private fine-tuning with ultra-low-parameter adapters.

The remainder of this paper is organized as follows. Section 2 provides overview of the related work. In Section 3, we establish the

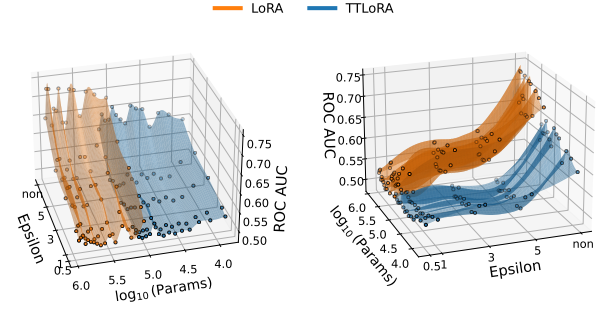


Figure 1: Attack AUC 3D surface on Enron dataset (two views). LoRA shows significant variation in attack AUC (lower is better) across epsilon whereas TTLLoRA maintains a relatively flat surface near the 50% random-guess baseline in private setting (non here means non-private setting).

necessary preliminaries by reviewing Tensor Train (TT) decomposition, detailing how TTLLoRA employs TT factorization to construct parameter-efficient adapters, and the challenge of per-example gradient computation of TTLLoRA in Differential Privacy. In Section 4, we introduce TTLLoRA-DP framework; here, we describe our primary technical contribution: an extension of the ghost clipping algorithm to TT-cores. Section 5 provides a rigorous empirical analysis of TTLLoRA-DP, evaluating its resilience against membership inference attacks and its utility-privacy trade-offs. Finally, Section 6 and 7 highlights the discussion of broader impacts and concluding remarks.

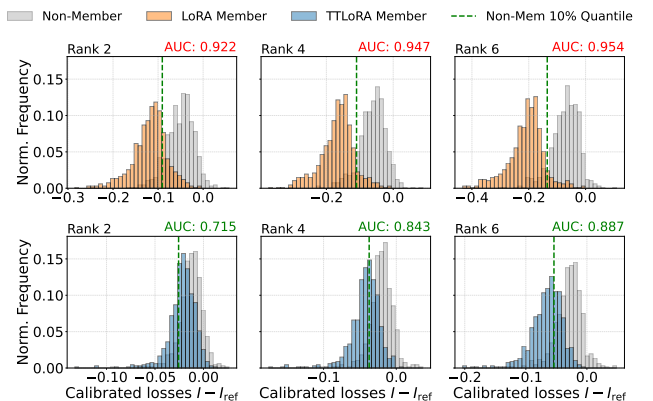


Figure 2: Calibrated loss distributions for MIA leakage (Enron) under non-private setting. Histograms show $\mathcal{L}(x; \theta_{\text{peft}}) - \mathcal{L}(x; \theta_{\text{ref}})$ for members and non-members at ranks 2/4/6 for LoRA and TTLLoRA; dashed line marks the 10% non-member quantile used for fixed-FPR evaluation. Larger separation implies higher AUROC and stronger leakage.

¹<https://github.com/Emory-AIMS/PreCurious>

2 Related Work

Parameter-Efficient Fine-Tuning (PEFT). PEFT methods adapt large pretrained models by updating only a small subset of parameters, reducing training and deployment costs. Among these methods [12, 17, 19], LoRA has become the widely adopted standard due to its simplicity, factorizing weight updates into two low-rank matrices [13]. However, LoRA imposes a fundamental *parameter floor*: the two-factor matrix structure enforces a minimum parameter count per adapted layer, limiting scalability in ultra-low-parameter regimes.

This has motivated *structured* PEFT parameterizations that further constrain the update space while retaining expressivity. Tensor-based approaches address this limitation by introducing stronger structural constraints. LoRETTA uses tensor-train (TT) decomposition [27] to reduce trainable parameters beyond conventional low-rank designs [34]. Closely related, TTLoRA and follow-up work explore TT-based parameterizations for fast, compressed fine-tuning and extensions to sparse MoE variants [2, 15]. Prior works establish tensor train's parameter compression capabilities but do not study its privacy implications. Our work focuses on an under-explored dimension: how TT structure (using TTLoRA), impacts *privacy leakage* and the *privacy–utility* frontier.

Privacy Leakage and Membership Inference. Fine-tuned language models are vulnerable to membership inference attacks (MIA), which infer whether a data point was used during training [30, 35]. A particularly relevant recent direction identifies new fine-tuning attack surfaces that exploit the *pretrained checkpoint*. *PreCurious* shows that an adversary can publish a crafted pre-trained model that later amplifies privacy leakage during a victim's fine-tuning, enabling strong black-box MIAs via calibrated losses [20]. Relatedly, *Privacy Backdoors* demonstrates that poisoning pretrained models can significantly increase membership leakage after fine-tuning, underscoring the risks of untrusted initialization checkpoints [32]. *Robust membership inference attack* (RMIA) models the null hypothesis in likelihood-ratio testing and leverages both reference models and population data to achieve high test power across the TPR–FPR curve [37]. Besides, our work studies PEFT privacy leakage and DP defenses in a fine-tuning pipeline, *PreCurious* provides a strong and practically motivated threat model for our evaluation.

Differential Privacy for Fine-Tuning LLM. Differential privacy (DP) [10] limits how much any single training example can influence a model's outputs, and in deep learning this is typically enforced by DP-SGD [1]. Despite its formal guarantees, the standard DP-SGD mechanism remains difficult to deploy for LLM. DP-SGD requires per-example gradient norm computation for clipping, which is memory and compute-intensive at LLM scale and has motivated specialized implementations such as ghost clipping and fast per-example clipping [1, 6, 11, 16, 18].

Even when training is made computationally feasible, the challenges arise from the fact that the magnitude of DP noise scales with the dimensionality of the trainable parameter space [1, 3, 7]. Reducing the number of parameters involved in training therefore directly improves both computational overhead and noise-induced utility degradation [22, 36]. PEFT methods address this issue by

restricting learning to a small subset of parameters, making them a natural substrate for private fine-tuning.

Differential Privacy Meets PEFT. Because PEFT restricts the trainable parameter space, this raises the question of whether PEFT *reduces privacy leakage* and whether it can improve DP utility. Recent works provide mixed but increasingly nuanced answers. On one hand, theoretical and empirical studies suggest that LoRA inherently acts like it injects noise-like effects into optimization and may partially resemble DP-SGD dynamics, with privacy behavior depending on rank and model dimensions [9, 23]. On the other hand, recent attacks specifically targeting LoRA fine-tuning show that LoRA-adapted models can remain largely vulnerable to MIAs [28], especially when the attacker leverages the publicly available pretrained model as a reference [20].

Several works explicitly study DP with PEFT and/or federated learning, proposing private low-rank adaptation mechanisms or improving LoRA-based federated training under privacy constraints [21, 31, 33]. Closest to our motivation, Ma et al. investigate memorization under DP parameter-efficient fine-tuning and show that PEFT can reduce leakage while retaining performance, but the role of *PEFT structure* is still not fully characterized [22]. In contrast to prior DP-PEFT studies that primarily focus on conventional LoRA, our work investigates whether *more structurally constrained* TT parameterized TTLoRA architecture can deliver stronger privacy–utility behavior and provides the first DP-SGD pipeline for TTLoRA.

3 Preliminaries

3.1 Tensor Train Decomposition

The Tensor Train (TT) decomposition [26, 27] compresses a high order n -dimensional tensor $\mathcal{T} \in \mathbb{R}^{I_1 \times I_2 \times \dots \times I_n}$ by factorizing it into a sequence of 3rd-order tensors called TT-cores. Specifically, each element of \mathcal{T} is computed by multiplying the corresponding slices of these cores as:

$$\mathcal{T}(i_1, i_2, \dots, i_n) = G_1[:, i_1, :] \cdot G_2[:, i_2, :] \cdots G_n[:, i_n, :] \quad (1)$$

where $G_k \in \mathbb{R}^{r_{k-1} \times I_k \times r_k}$ are the TT-cores and r_0, r_1, \dots, r_n are the TT-ranks (with $r_0 = r_n = 1$). This reduces storage complexity from $\mathcal{O}(\prod I_k)$ to $\mathcal{O}(\sum r_{k-1} I_k r_k)$, enabling extremely compact parameterization.

3.2 TTLoRA Architecture

TTLoRA is fine-tuning method based on TT decomposition. TTLoRA applies TT decomposition directly to the weight update $\Delta W \in \mathbb{R}^{d_{\text{out}} \times d_{\text{in}}}$. By representing ΔW as a chain of tensor cores, it achieves two key goals: (i) drastically reduces the number of trainable parameters, thereby breaking the LoRA parameter floor [15], and (ii) introduces a structured compositional constraint that implicitly regularizes the adaptation [29], which we hypothesize contributes to improved privacy and robustness.

Factorization. The weight update $\Delta W \in \mathbb{R}^{d_{\text{out}} \times d_{\text{in}}}$ is factorized along both input and output dimensions as:

$$d_{\text{in}} = \prod_{k=1}^p m_k, \quad d_{\text{out}} = \prod_{\ell=1}^q n_{\ell} \quad (2)$$

The adapter is then represented using $(p+q)$ TT-cores: input cores $G_k \in \mathbb{R}^{r_{k-1} \times m_k \times r_k}$ and output cores $G_\ell \in \mathbb{R}^{r_{p+\ell-1} \times n_\ell \times r_{p+\ell}}$, with boundary ranks $r_0 = r_{p+q} = 1$ and internal ranks typically set uniformly to r . To illustrate, consider GPT-2's attention weight of size $768(d_{out}) \times 2304(d_{in})$, which can be factorized into $[64, 4, 3] \times [3, 3, 4, 64]$. With TT-rank $r = 2$, the output TT-cores can be represented as $[1, 64, 2]$, $[2, 4, 2]$, and $[2, 3, 2]$ whereas the input cores as $[2, 3, 2]$, $[2, 3, 2]$, $[2, 4, 2]$, and $[2, 64, 1]$. In practice, the key hyperparameters controlling TTLoRA are the TT-rank r , the chosen factorization (TT-shape) of input and output dimensions, and the scaling factor α . During the forward pass, the input activation tensor is sequentially contracted with the input cores (compressing information into the rank dimension) and then expanded through the output cores. More details about tensor operations can be found in Section 4.1–4.4.

3.3 Differential Privacy and Challenges

Differential Privacy (DP) [10] provides a rigorous framework to bound privacy leakage from training data. A randomized mechanism \mathcal{M} satisfies (ϵ, δ) -DP if, for any two adjacent datasets D and D' differing in a single record, and any measurable set S :

$$\Pr[\mathcal{M}(D) \in S] \leq e^\epsilon \Pr[\mathcal{M}(D') \in S] + \delta \quad (3)$$

While DP offers formal privacy guarantees, applying it to LLM fine-tuning is challenging. Standard DP-SGD requires three key steps: (i) computing per-example gradient norms, (ii) clipping each gradient to a fixed norm to bound sensitivity, and (iii) adding calibrated noise to the aggregated gradients before updating the model. Computing exact per-example gradient norms for clipping is memory and compute intensive at LLM scale, especially for structured adapters. Ghost clipping [18] addresses the computational bottleneck by avoiding materialization of full per-example gradients, enabling efficient DP-SGD.

The Challenge for TTLoRA: Existing ghost clipping implementations² support standard layers (e.g., linear, convolutional, embeddings) and LoRA-style adaptation, but do not handle TTLoRA's chained TT-core parameterization. In TTLoRA, the weight update is represented implicitly as a product of small TT-cores and applied to an input via sequential core contractions. As a result, applying standard ghost clipping would require explicitly forming ΔW (or full per-example gradients), which is memory-prohibitive and negates the efficiency benefits of PEFT. The core mismatch is therefore structural: the per-example Jacobians needed for clipping are distributed across the TT-cores rather than associated with a single matrix parameter. To resolve this, we extend ghost clipping to TTLoRA by performing sequential contraction/expansion with cached states, enabling exact per-example gradient norm computation without exploding memory (more details in Section 4).

4 Extending Ghost Clipping for TTLoRA-DP

This section presents our extension of ghost clipping to enable efficient DP-SGD for TTLoRA. The central challenge is computing per-example gradient norms $\|\nabla_\theta \ell_i\|_2$ (where ℓ_i is per-example

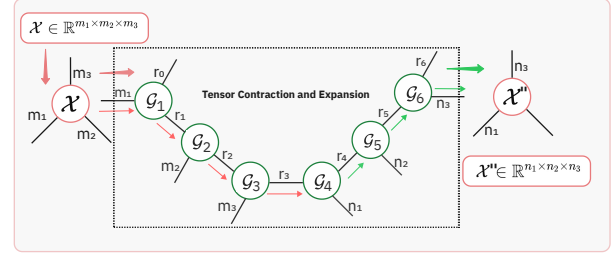


Figure 3: TTLoRA Architecture: Forward Pass Tensor Contraction and Expansion with Input tensor. Red arrow indicates the contraction while green arrow indicates the expansion of the intermediate input activation

loss)—required for gradient clipping—when the trainable parameters are not a single linear weight matrix but a sequence of Tensor Train (TT) cores.

To address this, we express the TTLoRA forward and backward passes as structured tensor contractions, cache intermediate contraction states, and reuse them to compute *exact* per-example gradient norms without materializing per-example gradient tensors. This preserves DP-SGD privacy guarantees while retaining the computational advantages of ghost clipping.

We proceed in stages. Section 4.1 introduces notation for TTLoRA-adapted layers and the forward computation. Section 4.2 describes reshaping input activation to match the TT factorization. Sections 4.3 and 4.4 detail the TTLoRA forward pass as a sequence of input contractions and output expansions, during which we cache intermediate states. Section 4.5 then shows how these cached states enable efficient per-example gradient norm calculation across TT-cores. Finally, Section 4.6 integrates the resulting norms into the ghost clipping and gradient update passes, enabling DP-SGD for TTLoRA without excessive memory overhead.

4.1 Notation

Here, we introduce the notation for TTLoRA-adapted layers and the overall forward computation. Let $x \in \mathbb{R}^{B \times S \times d_{in}}$ be a mini-batch input activation of B sequences of length S . A frozen base linear layer interacting with the input x produces:

$$y_{\text{base}}(x) = x W^\top, \quad W \in \mathbb{R}^{d_{out} \times d_{in}}.$$

TTLoRA augments this frozen base layer with a trainable TT adapter $f_{\text{TT}} : \mathbb{R}^{d_{in}} \rightarrow \mathbb{R}^{d_{out}}$, while all base model parameters remain fixed.

$$y(x) = y_{\text{base}}(x) + \alpha f_{\text{TT}}(x). \quad (4)$$

4.2 Input Reshaping

TTLoRA parameterizes the weight update using TT decomposition, which operates over 3rd-order tensor cores rather than flat vectors. To align the input activations with this structured parameterization, each input vector must first be reshaped into a tensor whose dimensions match the TT factorization of the input cores. This reshaping step is purely structural—it does not change the input

²<https://github.com/lxuechen/private-transformers>

values—but enables efficient tensor contractions with TT-cores in the subsequent forward and backward passes.

Let $\mathbf{X} \in \mathbb{R}^{B \times S \times d_{\text{in}}}$ denote a mini-batch of B sequences of length S , and let $x_{b,t} \in \mathbb{R}^{d_{\text{in}}}$ denote the input vector at batch index b and token position t . Each input vector is reshaped into a p -way tensor matching the factorization $d_{\text{in}} = \prod_{k=1}^p m_k$. Formally,

$$X_{\text{tensor}} \in \mathbb{R}^{B \times S \times m_1 \times \dots \times m_p}, \quad (5)$$

where the slice $X_{\text{tensor}}(b, t, :, :, \dots)$ corresponds to the tensorized form of $x_{b,t}$. This reshaping aligns the input activations with the TT factorization of the adapted weight in TTLoRA.

4.3 Contracting Input Factors

We next contract the reshaped input activation with the TT input cores. This step progressively aggregates input dimensions (see Fig.3) while introducing TT rank dimensions, and critically, allows us to cache intermediate activation states for further steps.

We now describe the forward pass for a single token $x_{b,t} \in \mathbb{R}^{d_{\text{in}}}$ from batch index b and sequence position t . After reshaping $x_{b,t}$ into a p -way tensor with dimensions (m_1, \dots, m_p) , we initialize the contraction state:

$$S_0(b, t) = x_{b,t} \in \mathbb{R}^{r_0 \times m_p \times \dots \times m_1}, \quad r_0 = 1.$$

We include the trivial rank dimension $r_0 = 1$ to simplify notation for the subsequent contractions. For $k = 1, \dots, p$, the input contraction between input activation with input TT-cores proceeds sequentially as:

$$S_k(b, t) = \sum_{a=1}^{r_{k-1}} \sum_{m=1}^{m_k} S_{k-1}(b, t)(a, \dots, m) \times G_k(a, m, \cdot) \quad (6)$$

where $G_k \in \mathbb{R}^{r_{k-1} \times m_k \times r_k}$ denotes the k -th input TT-core and $S_k(b, t) \in \mathbb{R}^{r_k \times m_{k-1} \times \dots \times m_1}$ denotes the k -th intermediate activation state. We cache each pre-core state $S_{k-1}(b, t)$, which is later reused during per-example backpropagation to compute gradient norms. After contracting all p input cores, the resulting state $S_p(b, t) \in \mathbb{R}^{r_p}$ provides a compact representation of the input under the TTLoRA adapter.

4.4 Expanding Output Factors

After contracting all input factors, we expand the representation through the output TT-cores to generate the output dimensions (see Fig. 3). This mirrors the input contraction process and similarly stores intermediate states needed for per-example gradient computation. The contracted state $S_p(b, t)$ is mapped to the output space using the q output TT-cores $\tilde{G}_\ell \in \mathbb{R}^{r_{p+\ell-1} \times n_\ell \times r_{p+\ell}}$. We initialize

$$T_0(b, t) = S_p(b, t) \in \mathbb{R}^{r_p}.$$

For $\ell = 1, \dots, q$, the expansion proceeds sequentially as

$$T_\ell(b, t) = \sum_{a=1}^{r_{p+\ell-1}} T_{\ell-1}(b, t)(a, \dots) \tilde{G}_\ell(a, \cdot, \cdot) \quad (7)$$

where $T_\ell(b, t) \in \mathbb{R}^{r_{p+\ell-1} \times n_1 \times \dots \times n_\ell}$, and we again cache each pre-core state $T_{\ell-1}(b, t)$. After processing all output cores, the final TT rank satisfies $r_{p+q} = 1$, yielding

$$T_q(b, t) \in \mathbb{R}^{n_1 \times \dots \times n_q}$$

Algorithm 1 Ghost Clipping for TTLoRA

Require: Batch $\{x_b\}_{b=1}^B$, clipping threshold C , noise multiplier σ

- 1: **Forward Pass:** Compute outputs $\{y_b\}$, cache states $\{S_{(k)}\}$
- 2: **Loss Computation:** Compute \mathcal{L} , get upstream $\{\Delta_b\}$
- 3: **First Backward (Norm) Pass:**
- 4: **for** $b = 1$ to B **do**
- 5: Compute per-example gradients via equations (8), (10)
- 6: Accumulate $\|g_b\|_2^2$ (discard individual gradients)
- 7: **end for**
- 8: **Compute Clipping Coefficients:** $c_b = \min(1, C/\|g_b\|_2)$
- 9: **Reweight Loss:** $\tilde{\ell}_b = c_b \cdot \ell_b$
- 10: **Second Backward (Gradient) Pass:**
- 11: **Loss backward** assigns clipped gradients to parameters
- 12: **for** each TT-core parameter tensor $\theta \in \{G_k, \tilde{G}_\ell\}$ **do**
- 13: $\bar{g}_\theta \leftarrow \sum_{b=1}^B c_b \cdot g_{\theta,b}$
- 14: $\tilde{g}_\theta \leftarrow \bar{g}_\theta + \mathcal{N}(0, \sigma^2 C^2 I)$
- 15: **end for**
- 16: **return** Noisy gradients $\{\tilde{g}_\theta\}$

Flattening the output modes produces the adapter output $f_{\text{TT}}(x_{b,t}) \in \mathbb{R}^{d_{\text{out}}}$, which is combined with the frozen base layer as

$$y(x_{b,t}) = x_{b,t} W^\top + \alpha f_{\text{TT}}(x_{b,t})$$

4.5 Per-Sample Backpropagation in TT-Cores

Having expanded the input through the output TT-cores, we now compute per-sample gradients with respect to each TT-core entry. Let $\mathcal{L} = \frac{1}{BS} \sum_{b,t} \ell(y_{b,t}, \text{label}_{b,t})$ denote the training loss. Autograd provides the upstream gradient for each token:

$$\Delta(b, t) = \frac{\partial \mathcal{L}}{\partial y_{b,t}} \in \mathbb{R}^{d_{\text{out}}}$$

Only the TT-adapter path receives the scaled gradient $\alpha \Delta$, which is reshaped to match the output tensor form:

$$\alpha \Delta(b, t) \xrightarrow{\text{reshape}} C_q(b, t) \in \mathbb{R}^{r_{p+q} \times n_1 \times \dots \times n_q}, \quad r_{p+q} = 1$$

which matches T_q . We now propagate per-example gradients right-to-left through the output cores and then through the input cores, reusing cached forward states. Following fast per-example gradient clipping [16], we compute per-token gradients in factored form as (upstream) \times (activation), and then apply this principle to TT-core contractions using cached states.

$$\left(\frac{\partial \mathcal{L}}{\partial W_{i,j}} \right) = \frac{\partial \mathcal{L}}{\partial Y_i} \cdot X_j$$

4.5.1 Gradients w.r.t. output cores \tilde{G}_ℓ . Let $T_{\ell-1}(b, t)$ be the pre-core state stored in the forward pass before contracting it with \tilde{G}_ℓ . The per-sample, per-token gradient is:

$$\frac{\partial \ell_{b,t}}{\partial \tilde{G}_\ell(a, n, b')} = \sum_{\text{context}} C_\ell(b, t)[b', \dots, n, \dots] \cdot T_{\ell-1}(b, t)[a, \dots] \quad (8)$$

which has shape $r_{p+\ell-1} \times n_\ell \times r_{p+\ell}$. Here, context denotes the product of all remaining indices in n_1, \dots, n_q except n_ℓ (and any rank indices implied by the current state). Backpropagating to the input of core

ℓ , which we store as the upstream gradient for the next core, yields:

$$C_{\ell-1}(b, t)[a, \dots] = \sum_{n, b'} C_\ell(b, t)[b', \dots, n, \dots] \cdot \tilde{G}_\ell(a, n, b') \quad (9)$$

4.5.2 Gradients w.r.t. input cores G_k . After processing all output cores, we obtain $C_0(b, t) \in \mathbb{R}^{rp}$, the upstream for the input cores. For $k = p, p-1, \dots, 1$, let the forward pre-core state be $S_{k-1}(b, t)$ and $U_k(b, t)$ be the current upstream (gradient w.r.t. S_k). Then per-sample, per-token gradient is,

$$\frac{\partial \ell_{b, t}}{\partial G_k(a, m, b')} = \sum_z U_k(b, t)[b', z] \cdot S_{k-1}(b, t)[a, z, m] \quad (10)$$

and the upstream for the next core, which we store for the upcoming core, is:

$$U_{k-1}(b, t)[a, z, m] = \sum_{b'=1}^{r_k} U_k(b, t)[b', z] \times G_k(a, m, b') \quad (11)$$

For $k > 1$, U_{k-1} matches the shape of S_{k-1} and becomes the next upstream.

4.6 Ghost Clipping on Per-Sample Gradients

To efficiently enforce per-example ℓ_2 clipping while keeping memory usage manageable, we implement a two-pass procedure from Ghost Clipping. Algorithm 1 summarizes this procedure, showing how forward caching, per-example norm computation, and a second backward pass with gradient scaling and noise addition are orchestrated.

With per-sample gradients for all TT-core parameters computed in above sections, we now enforce ℓ_2 -norm bounds for DP. This ensures that each example contributes at most C to the gradient, which is critical for differential privacy and for preventing outlier gradients from destabilizing training. Let θ be any trainable parameter (a TT-core entry). For example (b, t) the per-sample gradient is $\nabla_\theta \ell_{b, t}$ computed by (8) and (10). For each parameter, we accumulate each parameter's per example norm contribution across tokens and cores as:

$$g_\theta^{(b)} = \left\| (\nabla_\theta \ell_{b,1}, \dots, \nabla_\theta \ell_{b,S}) \right\|_2 \quad (\text{aggregated over tokens})$$

and combine all parameters to form a per-example global norm:

$$\|g_\theta\|_2 = \left(\sum_\theta (g_\theta^{(b)})^2 \right)^{1/2}$$

Clipping coefficients are then applied in a second backward pass, scaling each example's contribution so that the overall per-example gradient is ℓ_2 -bounded by C as (small value $\tau \sim 10^{-6}$ is added to avoid division by 0):

$$c_b = \min \left\{ 1, \frac{C}{\|g_\theta\|_2 + \tau} \right\}$$

Memory Complexity: Materializing per-example gradients requires $\mathcal{O}(B \cdot |\theta|)$ memory where $|\theta|$ is the parameter count. Our ghost clipping implementation avoids storing per-example gradients and instead caches only TT contraction states requiring only $\mathcal{O}(BS \cdot r^2 \cdot (p + q))$ memory for cached states plus $\mathcal{O}(B)$ for per-example norms. In particular, memory does not scale with the size of the implicit matrix $\Delta W \in \mathbb{R}^{d_{\text{out}} \times d_{\text{in}}}$.

5 Analysis of Privacy–Utility Trade-offs in TT-LoRA

In this section, we evaluate TTLoRA's privacy–utility profile relative to LoRA and full fine-tuning (FFT) under both DP-SGD and non-private training. We first describe the model, datasets, PEFT configurations, and evaluation setup (Section 5.1), followed by the details about PreCurious attack protocol (Section 5.2). Furthermore, we systematically study TTLoRA's privacy–utility properties along three complementary dimensions:

- (1) **Utility under Differential Privacy:** We evaluate how DP-SGD affects language-modeling performance across privacy budgets, comparing privately trained TTLoRA, LoRA, and FFT (Sec. 5.3, Table 2, Fig. 4, 5).
- (2) **Membership Inference Vulnerability under DP:** We analyze how DP budgets influence susceptibility to PreCurious membership inference attack, highlighting TTLoRA's robustness relative to LoRA and FFT (Sec. 5.4, Table 3, Fig. 1, 6).
- (3) **Inherent Privacy Resilience without DP:** We examine TTLoRA's intrinsic privacy properties in a non-private setting, showing that even without DP, TTLoRA substantially reduces membership leakage while maintaining competitive utility (Sec. 5.5, Table 4, Fig. 2, 7).

Our experiments reveal three key insights: (1) under identical DP constraints, TTLoRA matches or improves utility relative to LoRA while using an order-of-magnitude fewer trainable parameters; (2) TTLoRA exhibits lower membership leakage preserving utility under DP training, remaining nearly flat as ϵ increases, whereas LoRA's leakage grows substantially; (3) under non-private training, TTLoRA exhibits substantially lower membership leakage in exchange of less utility cost; these findings suggest that TTLoRA's tensor-train structure can materially reduce the membership signal exploited by loss-based attacks.

5.1 Model and Dataset

Following prior works [20, 23], we fine-tune GPT-2 (124M) on two benchmark datasets containing confidential or sensitive content:

- **Enron Email Corpus** [14]: Corporate email communications released during the Enron investigation, containing sensitive business discussions.
- **Penn Treebank (PTB)** [24]: Wall Street Journal articles covering business and financial news.

We evaluate utility using validation perplexity (PPL; lower is better) and privacy leakage using attack AUC-ROC (lower is better) along with different recall rates at variable False Positive Rates (FPR) (lower is better).

Fine-Tuning Methods: We compare three approaches:

- **Full Fine-Tuning (FFT):** All 124M parameters trainable; Learning rate $1e^{-4}$
- **LoRA:** Adapted on attention weights (c_{attn}) and projection weights (c_{proj}) of all 12 layers with ranks $r \in \{2, 4, 6, 8, 10, 12, 14, 16\}$, yielding 110.6K–884.7K trainable parameters; Learning rate $5e^{-4}$
- **TTLoRA:** Tensor train adapters on the same weights as LoRA adaptation with matching ranks, yielding 7.6K–144.4K trainable parameters. The TT-factorization uses [64, 4, 3]

factors for 768 and $[64, 4, 3, 3]$ factors for 2304 and factorize c_{attn} with dimension 768×2304 and c_{proj} with dimension 768×768 ; Learning rate $5e^{-3}$

Privacy Configurations: We train under four privacy budgets $\epsilon \in \{0.5, 1.0, 3.0, 5.0\}$ and report a non-private baseline (DP disabled). For DP runs, we use $\delta = N^{-1.1}$ where N is the number of training samples, consistent with prior practice. For DP training, we use private-transformers³ [18] with our TTLoRA ghost clipping extension with effective batch size 32, and tune the noise multiplier to achieve the target ϵ over the training steps using Renyi DP accounting method [25].

Evaluation Metrics: We measure privacy and utility metrics:

- **Utility:** Validation perplexity (PPL, lower is better),
- **Privacy Leakage:** We evaluate membership inference attack success using the calibrated loss-threshold method PreCurious (more details in section 5.2) [20]. We measure: (1) *Attack AUC*: area under the ROC curve (50% = random guess), (2) *TPR@FPR=1%*: True Positive Rate at False Positive Rate of 0.01, (3) *TPR@FPR=0.1%*: True Positive Rate at False Positive Rate of 0.001, (4) *TPR@FPR=0.01%*: True Positive Rate at False Positive Rate of 0.0001.

Ranks Configuration: All experiments for both LoRA and TTLoRA are conducted using even ranks $r \in \{2, 4, \dots, 16\}$, and we report rank-averaged results in Tables 2, 3, and 4. This range corresponds to the low to moderate rank regime commonly explored in prior PEFT studies [4, 13, 15, 22], where adapters provide substantial parameter efficiency without approaching the behavior of full fine-tuning. Larger ranks increasingly saturate utility while substantially increasing the number of trainable parameters and exhibit increasing vulnerability towards MIA leakage (see Table 1), whereas very small ranks often suffer from unstable training and degraded performance.

To ensure that our conclusions are not sensitive to a particular rank choice, we average results across this range. This reporting strategy mitigates variance due to rank-specific effects and enables a robust comparison between LoRA and TTLoRA. Full rank-wise results for Section 5.3, 5.4, 5.5 are provided in the appendix due to space constraints.

5.2 PreCurious Membership Inference Attack

Following the PRECURIOUS threat model [20], we consider a prominent black-box adversary who (i) publishes a crafted pre-trained checkpoint (ii) later queries the victim’s released fine-tuned model. The attack can be viewed in three stages:

Crafting: The adversary **warms-up** a benign pre-trained model θ_{benign} (fully fine-tune for some epochs) on an auxiliary corpus (D_{aux} : drawn from the same distribution as the victim’s private fine-tuning data but disjoint from it) to obtain an adversarial initialization and later uses as a reference model θ_{ref} .

Fine-tuning: The victim downloads the released checkpoint θ_{ref} , attaches PEFT modules, fine-tunes on private data D_{train} and releases θ_{peft} model,

³<https://github.com/lxuechen/private-transformers>

Table 1: Comparison of attack metrics (AUC, FPR@1%, FPR@0.01%) and utility (PPL) for LoRA, TTLoRA, and FFT on the Enron dataset under non-private (no DP) setting. Lower ↓ is better. Bold orange (LoRA) and blue (TTLoRA) indicate best individual performance; bold black indicates best average performance; gray highlighted rows correspond to equivalent parameter count configurations.

Method	Rank	Params	PPL	AUC	FPR@1%	FPR@0.01%
LoRA	2	110.6k	17.74	92.23%	25.34%	0.45%
	4	221.2k	17.59	94.71%	35.23%	0.90%
	6	331.8k	17.41	95.41%	36.28%	0.75%
	8	442.4k	17.62	93.89%	37.33%	1.95%
	10	553.0k	17.36	96.04%	27.29%	1.65%
	12	663.6k	17.38	95.70%	37.78%	2.40%
	14	774.1k	17.29	95.95%	28.49%	1.35%
	16	884.7k	17.32	95.35%	40.03%	1.50%
Avg.	–	497.7k	17.46	94.91%	33.47%	1.37%
TTLoRA	2	7.6k	18.35	71.49%	4.20%	0.45%
	4	18.2k	18.23	84.35%	5.25%	1.65%
	6	31.8k	18.11	88.72%	13.94%	1.80%
	8	48.4k	17.97	92.99%	21.59%	0.75%
	10	67.9k	18.04	92.30%	18.74%	1.95%
	12	90.4k	17.90	93.85%	19.94%	0.30%
	14	115.9k	17.97	91.65%	22.04%	1.65%
	16	144.4k	17.83	94.10%	23.84%	0.30%
Avg.	–	65.6k	18.05	88.68%	16.19%	1.11%
FFT	–	124.04M	16.45	96.63%	26.24%	4.35%

Inferring: The adversary performs membership inference using only loss queries. We split the original training corpus into three equal partitions ($D_{\text{aux}}, D_{\text{train}}, D_{\text{non}}$) to mimic the real-world scenario, where D_{non} serves as a non-member calibration set. At inference time, we compute a calibrated membership score using the crafted reference model θ_{ref} trained on D_{aux} as:

$$s_{\text{ref}}(x) = \mathcal{L}(x; \theta_{\text{peft}}) - \mathcal{L}(x; \theta_{\text{ref}}), \quad (12)$$

where \mathcal{L} is the per-sample loss. Given a target false-positive rate α , we set the threshold τ_α as the largest value that keeps the FPR on D_{non} below α such that $\Pr_{x \sim D_{\text{non}}} [s_{\text{ref}}(x) \leq \tau_\alpha] = \alpha$ and $\text{TPR}(\alpha) = \Pr_{x \sim D_{\text{train}}} [s_{\text{ref}}(x) \leq \tau_\alpha]$. We summarize attack effectiveness using ROC-AUC by treating members as label 1 and non-members as label 0, and using scores $-s_{\text{ref}}(x)$ so that lower calibrated loss corresponds to higher membership likelihood.

5.3 Differentially Private (DP) Training: Privacy–Utility Trade-offs

We evaluate the utility of DP fine-tuning under DP-SGD on Enron and PTB datasets. Unlike our attack evaluation protocol (which splits the corpus into $D_{\text{aux}}, D_{\text{train}}, D_{\text{non}}$), here we fine-tune on the *full* training set to isolate the privacy–utility impact of DP-SGD. We adapt a pretrained GPT-2 checkpoint using either LoRA or TTLoRA and train for 15 epochs under privacy budgets $\epsilon \in \{0.5, 1.0, 3.0, 5.0\}$, selecting the best validation checkpoint (by validation PPL) for each

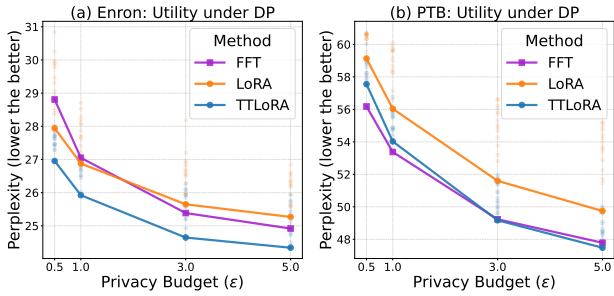


Figure 4: Pareto Frontier: Best utility extracted among multiple configurations under differential privacy. TTLoRA achieves better perplexity than LoRA at all privacy budgets, with the advantage strongest at stricter (lower ϵ) settings.

ϵ for reporting. For LoRA and TTLoRA, we extract results for even ranks $r \in \{2, 4, \dots, 16\}$; Table 2 reports results averaged over ranks, while Table 6 in appendix provides the full rank-wise breakdown.

The non-private column in Table 2 is obtained by running the DP training pipeline with DP disabled, and is not directly comparable to the non-private column of Table 4 which is measured under the attack pipeline and uses a different data split and warm-start procedure following the PreCurious protocol.

Table 2: Perplexity (lower is better) under DP averaged over performance at even ranks spanning 2 to 16. TTLoRA achieves better utility than LoRA at all privacy budgets.

Method	Params	Privacy Budget (ϵ)				Non-Priv.
		0.5	1.0	3.0	5.0	
<i>Enron Dataset</i>						
FFT	124.0M	28.81	27.05	25.38	24.92	14.31
LoRA (avg.)	497.7K	29.29	27.62	26.64	26.44	18.79
TTLoRA (avg.)	65.6K	27.52	26.55	25.37	24.99	20.14
<i>PTB Dataset</i>						
FFT	124.0M	56.18	53.38	49.23	47.79	19.75
LoRA (Avg.)	497.7K	60.41	58.59	54.75	53.81	28.86
TTLoRA (Avg.)	65.6K	58.47	55.39	50.61	48.71	31.45

We observe that TTLoRA improves DP utility despite fewer parameters. Across all privacy budgets, TTLoRA achieves lower (better) perplexity than LoRA on both datasets while using substantially fewer trainable parameters (65.6K vs. 497.7K on average). On Enron, TTLoRA improves over LoRA at every ϵ : e.g., at $\epsilon=0.5$, TTLoRA attains 27.52 PPL vs. 29.29 for LoRA, and at $\epsilon=3.0$ it attains 25.37 vs. 26.64. On PTB, the gap is even larger: at $\epsilon=5.0$, TTLoRA achieves 48.71 vs. 53.81 for LoRA. Figure 4 (which plots the best utility among 16 ranks configurations) visualizes the same trend as a function of ϵ : utility improves monotonically as the privacy budget increases (less noise), and TTLoRA consistently traces a curve closer to or even better than FFT than LoRA.

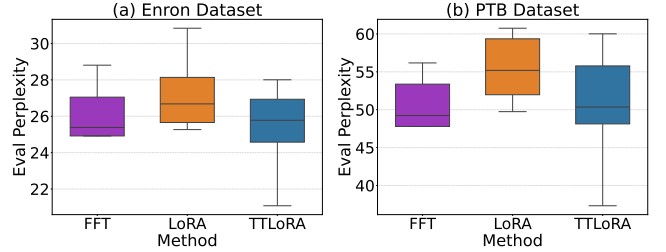


Figure 5: Overall utility comparison over different rank configurations for LoRA and TTLoRA along with FFT under DP training with Enron and PTB datasets

Relationship to full fine-tuning (FFT). FFT remains the strongest non-private baseline in perplexity, but under DP-SGD its advantage narrows substantially. On Enron, TTLoRA matches or slightly exceeds FFT at moderate privacy (25.37 vs. 25.38 at $\epsilon=3.0$), and outperforms FFT at strict privacy (27.52 vs. 28.81 at $\epsilon=0.5$), despite using orders of magnitude fewer trainable parameters. On PTB, FFT yields the best perplexity across budgets, but TTLoRA closes most of the gap relative to LoRA (e.g., at $\epsilon=5.0$, TTLoRA is within ≈ 0.92 PPL of FFT, whereas LoRA is ≈ 6.02 PPL worse). The box-plot summary in Figure 5 further corroborates this: TTLoRA exhibits consistently lower median perplexity and reduced dispersion compared to LoRA under DP.

5.4 DP Training under Attack: MIA at Varying Privacy Budgets

We evaluate privacy leakage under differentially private (DP) fine-tuning using the *PreCurious* membership inference attack [20]. For each dataset, we partition the original training split into three equal parts: an auxiliary subset D_{aux} for warm-up, a member subset D_{train} used for DP fine-tuning, and a disjoint non-member subset D_{non} used only for attack calibration. We warm up a GPT-2 base model for 2 epochs on D_{aux} to obtain an adversarially-initialized checkpoint, and set the resulting model as the reference θ_{ref} . We then adapt the model with either LoRA or TTLoRA and fine-tune the PEFT parameters on D_{train} for 15 epochs with DP-SGD, targeting privacy budgets $\epsilon \in \{0.5, 1.0, 3.0, 5.0\}$ (fixed δ and clipping configuration across methods).

Following *PreCurious*, we compute calibrated membership scores based on reference vs. adapted losses using equation 12 and summarize attack strength using ROC-AUC and fixed-FPR operating points (here reported as FPR@10%). For each (method, rank, ϵ) configuration, we report the *best epoch* (based on validation perplexity) and extract the result for all ϵ for the same epoch) and aggregate results over even ranks $r \in \{2, 4, \dots, 16\}$ as presented in Table 3 while Table 7 and 8 in appendix present the detailed rank-wise performance for Enron and PTB datasets.

TTLoRA is consistently harder to infer under DP, and the advantage widens as ϵ increases. Across both Enron and PTB, TTLoRA yields uniformly lower attack AUC than LoRA at the same privacy budget. On Enron, LoRA's rank-averaged AUC increases sharply as the privacy constraint relaxes (52.49% \rightarrow 58.43% from

Table 3: Comparison of attack metrics (AUC↓ and TPR@FPR=10%↓) and utility (PPL↓) for LoRA, TTLoRA (averaged over ranks 2–16), and FFT across Enron and PTB datasets under DP-SGD. Lower is better for AUC, TPR@FPR=10%, and PPL.

Method	$\epsilon = 0.5$			$\epsilon = 1.0$			$\epsilon = 3.0$			$\epsilon = 5.0$		
	AUC	PPL	FPR@10%									
Enron Dataset												
FFT	54.00%	21.48	11.24%	55.06%	21.25	11.84%	57.66%	20.99	15.29%	59.04%	20.90	15.74%
LoRA (avg.)	52.49%	20.72	11.14%	53.72%	20.72	12.11%	56.99%	20.71	14.91%	58.43%	20.71	15.89%
TTLoRA (avg.)	51.36%	20.72	10.66%	51.48%	20.72	10.87%	51.76%	20.72	11.19%	52.04%	20.72	11.23%
PTB Dataset												
FFT	50.09%	32.52	10.63%	51.74%	32.36	11.49%	56.32%	32.05	15.23%	59.28%	31.90	19.25%
LoRA (avg.)	52.62%	31.51	10.88%	53.57%	31.51	12.18%	56.55%	31.51	15.27%	58.58%	31.51	18.14%
TTLoRA (avg.)	51.62%	31.52	9.41%	51.65%	31.52	9.34%	51.82%	31.51	9.45%	52.19%	31.51	9.84%

$\epsilon = 0.5$ to 5), while TTLoRA remains close to the 50% random-guess baseline and changes only marginally (51.36% → 52.04%). This produces a growing AUC gap from 1.13 points at $\epsilon = 0.5$ to 6.39 points at $\epsilon = 5$. A similar trend holds on PTB, where LoRA rises from 52.62% to 58.58%, whereas TTLoRA stays near 51.62–52.19%. Figure 6 visualizes this effect and reports the average AUC reduction achieved by TTLoRA across ϵ (3.7 points on Enron and 3.5 points on PTB).

Fixed-FPR operating points show increasing separability for LoRA but near-constant leakage for TTLoRA. The same widening pattern appears under TPR@FPR = 10%. On Enron, LoRA’s TPR@10% increases from 11.14% to 15.89% as ϵ increases, whereas TTLoRA remains nearly flat (10.66% to 11.23%). On PTB, LoRA reaches 18.14% at $\epsilon = 5$, while TTLoRA stays below 10% across all budgets (9.34–9.84%). These results indicate that relaxing the privacy budget (adding less noise) significantly increases membership distinguishability for LoRA, but has limited effect for TTLoRA.

Utility is essentially matched in the attack-evaluation pipeline, so privacy gains are not driven by degraded accuracy. In the PreCurious setting, LoRA and TTLoRA achieve nearly identical rank-averaged perplexity and exhibit minimal sensitivity to ϵ (e.g., Enron \approx 20.71–20.72; PTB \approx 31.51–31.52 in Table 3). Therefore, the improved privacy of TTLoRA is not explained by a utility drop, but rather by reduced member/non-member separability in the calibrated loss space that the attacker exploits.

Overall, under identical DP budgets and the same attack protocol, TTLoRA provides a strictly improved privacy profile over LoRA while preserving essentially the same perplexity in this attack-evaluation regime.

5.5 Non-Private Baseline: Utility and MIA Vulnerability

We establish a non-private baseline by evaluating standard fine-tuning and PEFT adaptation under the PreCurious MIA protocol. Starting from a pretrained GPT-2 checkpoint, we warm-start the reference model on the auxiliary split D_{aux} for 5 epochs and then attach a PEFT module (LoRA or TTLoRA) to obtain the adapted model. The adapted model is fine-tuned on D_{train} for up to 200

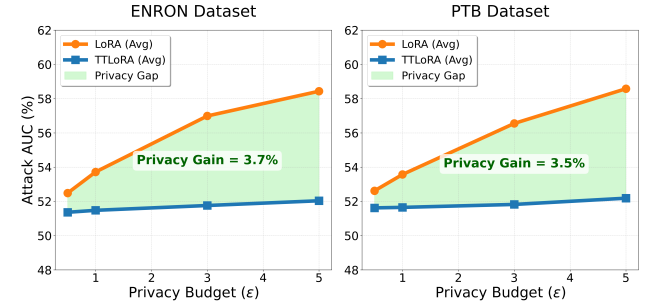


Figure 6: MIA AUC under PreCurious (rank-averaged). TTLoRA remains near the random-guess baseline (50%) across all ϵ , while LoRA becomes increasingly vulnerable as ϵ increases. Shaded region denotes the AUC gap (mean privacy gain: 3.7 points on Enron, 3.5 points on PTB).

epochs with early stopping (patience = 5) to get the stable and converged model for privacy analysis.

After convergence, we compute per-example losses on members (D_{train}) and non-members (D_{non}) and evaluate membership inference using the calibrated loss-gap score using equation 12. Table 4 summarizes average utility and attack metrics over even ranks $r \in \{2, 4, \dots, 16\}$ whereas Table 1 details the rank-wise performance and privacy analysis for Enron dataset (detailed table for PTB in appendix Table 5). Figure 7 visualizes the privacy–utility frontier. Complementarily, Figure 2 shows the calibrated loss distributions for members vs. non-members, where larger distributional gaps correspond to stronger membership signals and thus higher attack success.

Our results indicate that TTLoRA attains a distinctly improved privacy–efficiency trade-off compared to LoRA, achieving comparable language-modeling utility while substantially reducing membership leakage with substantially fewer trainable parameters. On Enron at rank $r=2$, TTLoRA uses only 7.6K trainable parameters (vs. 110.6K for LoRA; 14.5× fewer) and reaches a perplexity of 18.35 compared to 17.74 for LoRA, corresponding to only a 3.4% relative difference in PPL (see Table 1). At this comparable utility, TTLoRA substantially decreases attack effectiveness,

reducing attack ROC-AUC by 20.74 percentage points (92.23% for LoRA vs. 71.49% for TTLoRA) and reducing TPR at FPR=1% by 21.14 percentage points (25.34% for LoRA vs. 4.20% for TTLoRA). Aggregated over even ranks $r \in \{2, 4, \dots, 16\}$, TTLoRA achieves a lower mean attack AUC-ROC than LoRA (88.68% vs. 94.91%), i.e., a 6.2 percentage-point reduction. The low-FPR operating-point metric highlights an even larger privacy gain: TPR@FPR=1% decreases from 33.47% (LoRA) to 16.19% (TTLoRA), an absolute reduction of 17.28 percentage points. Consistent with these quantitative improvements, Figure 2 shows that TTLoRA yields substantially greater overlap between member and non-member calibrated loss distributions than LoRA, thereby weakening the separability signal exploited by membership inference attacks.

Table 4: Non-private fine-tuning: Utility (PPL \downarrow) and MIA vulnerability (AUC \downarrow and FPR \downarrow) averaged over even ranks (2-16) for LoRA and TTLoRA; \downarrow means lower is better.

Method	Params	PPL \downarrow	AUC \downarrow	FPR@1% \downarrow
<i>Enron Dataset</i>				
FFT	124.0M	16.45	96.63%	26.24%
LoRA (avg.)	497.7K	17.46	94.91%	33.47%
TTLoRA (avg.)	65.6K	18.05	88.68%	16.19%
<i>PTB Dataset</i>				
FFT	124.0M	23.15	99.15%	64.94%
LoRA (avg.)	497.7K	25.49	98.85%	32.51%
TTLoRA (avg.)	65.6K	26.66	97.17%	29.67%

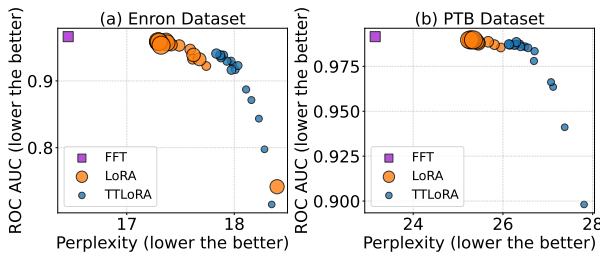


Figure 7: Privacy-utility tradeoff in non-private fine-tuning. Each point represents a rank configuration; marker size proportional to parameter count. TTLoRA achieves lower attack AUC (better privacy) with modest perplexity increase.

6 Discussion

Our results indicate that PEFT *architecture* not just can lower the parameter count but also can substantially shape the privacy–utility trade-off in LLM adaptation. Across Enron and PTB, TTLoRA consistently reduces membership inference vulnerability relative to LoRA, and this advantage persists both without DP and under DP-SGD across the evaluated privacy budgets and TT-ranks. Importantly, these privacy gains are achieved in a markedly smaller adapter regime: TTLoRA operates with roughly 10K–150K trainable

parameters, whereas LoRA requires roughly 100K–1,000K parameters over comparable rank ranges. A key takeaway is that TTLoRA appears to suppress the membership signal exploited by calibrated loss-based attacks. The tensor-train parameterization restricts the update space through a chained, compositional structure, which can act as a stronger inductive bias than a single low-rank factorization in LoRA. Empirically, this manifests as greater overlap between member and non-member calibrated loss distributions and near-random-guess attack AUC under DP for TTLoRA, even as ϵ increases. In contrast, LoRA’s leakage rises noticeably as the privacy budget relaxes, suggesting that additional capacity in a less constrained update space translates more directly into example-specific fitting. Under DP-SGD, TTLoRA’s structure may provide a second benefit: improved robustness to optimization noise. Because the update is distributed across multiple small cores, each constrained by TT-ranks and sequential contractions, the effective degrees of freedom are reduced and gradients are implicitly regularized. This can make the learning dynamics less sensitive to the perturbations introduced by clipping and Gaussian noise, helping TTLoRA retain (and in some settings improve) perplexity relative to LoRA at the same (ϵ, δ) .

Practical implications. These findings suggest that privacy preserving adaptation need not rely solely on tighter privacy budgets or stronger noise multipliers. Instead, selecting a PEFT parameterization with an appropriate structural constraint can materially reduce empirical leakage while maintaining competitive utility, and can do so in an ultra-low-parameter regime that is attractive for deployment.

Limitations. Our evaluation focuses on GPT-2 (124M), two language modeling datasets, and a strong loss-based black-box MIA (PreCurious). While PreCurious captures an important and practical threat model, it does not cover the full spectrum of privacy risks (e.g., data extraction or broader memorization behaviors). In addition, our utility metric is perplexity; downstream task performance and instruction-following behaviors may exhibit different trade-offs.

Future work. Several directions follow naturally from this study: (1) scaling TTLoRA-DP to larger modern LLMs (e.g., LLaMA-family and GPT-style models), where the adapter parameter savings and training-time efficiencies are even more consequential; (2) expanding evaluation beyond perplexity to downstream tasks and training regimes (instruction tuning, supervised fine-tuning, RLHF-style settings); (3) testing stronger and complementary privacy evaluations, including alternative MIAs, data extraction attacks, and memorization-oriented benchmarks; (4) combining TTLoRA-DP with orthogonal privacy techniques (e.g., federated learning or secure aggregation) to study end-to-end privacy in distributed settings; and (5) developing privacy accounting and algorithmic refinements that leverage TT structure—e.g., layer-wise clipping, structured noise, or tighter accounting under structural constraints—to further improve the privacy–utility frontier.

7 Conclusion

This work studies how PEFT architecture influences privacy leakage and utility under differentially private fine-tuning of language models. We establish TTLoRA as a structurally constrained PEFT approach and address the core systems challenge of enabling DP-SGD

for TT-adapters by extending ghost clipping with cached contraction states, making exact per-example norm computation practical for TT-core backpropagation.

Empirically, TTLoRA improves the privacy–utility trade-off across two datasets and multiple privacy budgets. Under DP training, TT-LoRA achieves consistently improved perplexity than LoRA at all evaluated ϵ values while using substantially fewer trainable parameters.

Under the PreCurious membership inference attack protocol, TTLoRA stays close to the random-guess baseline across privacy budgets and ranks, whereas LoRA becomes increasingly vulnerable as the privacy budget relaxes. These privacy gains are not driven by degraded utility in the attack-evaluation pipeline.

Overall, our results suggest that TT decomposition is not only a compression mechanism but also a principled architectural bias for privacy-preserving LLM adaptation. TTLoRA provides a practical route to improving DP utility while reducing empirical membership leakage relative to widely used PEFT baselines under comparable privacy constraints.

Acknowledgments

This research was funded by the Los Alamos National Laboratory (LANL) Laboratory Directed Research and Development (LDRD) program under grants 20250850ECR and 20240868PRD3 and supported by LANL’s Institutional Computing Program, and by the U.S. Department of Energy National Nuclear Security Administration under Contract No. 89233218CNA000001.

References

- [1] Martin Abadi, Andy Chu, Ian Goodfellow, H Brendan McMahan, Ilya Mironov, Kunal Talwar, and Li Zhang. 2016. Deep learning with differential privacy. In *Proceedings of the 2016 ACM SIGSAC conference on computer and communications security*. 308–318.
- [2] Afia Anjum, Maksim E Eren, Ismael Boureima, Boian Alexandrov, and Manish Bhattacharai. 2024. Tensor train low-rank approximation (tt-lora): Democratizing ai with accelerated llms. In *2024 International Conference on Machine Learning and Applications (ICMLA)*. IEEE, 583–590.
- [3] Raef Bassily, Adam Smith, and Abhradeep Thakurta. 2014. Private empirical risk minimization: Efficient algorithms and tight error bounds. In *2014 IEEE 55th annual symposium on foundations of computer science*. IEEE, 464–473.
- [4] Dan Biderman, Jacob Portes, Jose Javier Gonzalez Ortiz, Mansheej Paul, Philip Greengard, Connor Jennings, Daniel King, Sam Havens, Vitaliy Chiley, Jonathan Frankle, et al. 2024. Lora learns less and forgets less. *arXiv preprint arXiv:2405.09673* (2024).
- [5] Hannah Brown, Katherine Lee, Fatemehsadat Mireshghallah, Reza Shokri, and Florian Tramèr. 2022. What does it mean for a language model to preserve privacy?. In *Proceedings of the 2022 ACM conference on fairness, accountability, and transparency*. 2280–2292.
- [6] Zhiqi Bu, Jialin Mao, and Shiyun Xu. 2022. Scalable and efficient training of large convolutional neural networks with differential privacy. *Advances in Neural Information Processing Systems* 35 (2022), 38305–38318.
- [7] Mark Bun, Jonathan Ullman, and Salil Vadhan. 2014. Fingerprinting codes and the price of approximate differential privacy. In *Proceedings of the forty-sixth annual ACM symposium on Theory of computing*. 1–10.
- [8] Nicholas Carlini, Florian Tramer, Eric Wallace, Matthew Jagielski, Ariel Herbert-Voss, Katherine Lee, Adam Roberts, Tom Brown, Dawn Song, Ulrich Erlingsson, et al. 2021. Extracting training data from large language models. In *30th USENIX security symposium (USENIX Security 21)*. 2633–2650.
- [9] Soumi Das, Camila Kolling, Mohammad Aflah Khan, Mahsa Amani, Bishwamitra Ghosh, Qinyuan Wu, Till Speicher, and Krishna P Gummadi. 2025. Revisiting Privacy, Utility, and Efficiency Trade-offs when Fine-Tuning Large Language Models. *arXiv preprint arXiv:2502.13313* (2025).
- [10] Cynthia Dwork, Frank McSherry, Kobbi Nissim, and Adam Smith. 2006. Calibrating noise to sensitivity in private data analysis. In *Theory of cryptography conference*. Springer, 265–284.
- [11] Ian Goodfellow. 2015. Efficient per-example gradient computations. *arXiv preprint arXiv:1510.01799* (2015).
- [12] Neil Houlsby, Andrei Giurgiu, Stanislaw Jastrzebski, Bruna Morrone, Quentin De Laroussilhe, Andrea Gesmundo, Mona Attariyan, and Sylvain Gelly. 2019. Parameter-efficient transfer learning for NLP. In *International conference on machine learning*. PMLR, 2790–2799.
- [13] Edward J Hu, Yelong Shen, Phillip Wallis, Zeyuan Allen-Zhu, Yuanzhi Li, Shean Wang, Lu Wang, Weizhu Chen, et al. 2022. Lora: Low-rank adaptation of large language models. *ICLR* 1, 2 (2022), 3.
- [14] Bryan Klimt and Yiming Yang. 2004. The enron corpus: A new dataset for email classification research. In *European conference on machine learning*. Springer, 217–226.
- [15] Pradip Kunwar, Minh N Vu, Maanak Gupta, Mahmoud Abdelsalam, and Manish Bhattacharai. 2025. TT-LoRA MoE: Using Parameter-Efficient Fine-Tuning and Sparse Mixture-Of-Experts. In *Proceedings of the International Conference for High Performance Computing, Networking, Storage and Analysis*. 1332–1350.
- [16] Jaewoo Lee and Daniel Kifer. 2021. Scaling up differentially private deep learning with fast per-example gradient clipping. *Proceedings on Privacy Enhancing Technologies* (2021).
- [17] Brian Lester, Rami Al-Rfou, and Noah Constant. 2021. The power of scale for parameter-efficient prompt tuning. *arXiv preprint arXiv:2104.08691* (2021).
- [18] Xuechen Li, Florian Tramer, Percy Liang, and Tatsunori Hashimoto. 2021. Large language models can be strong differentially private learners. *arXiv preprint arXiv:2110.05679* (2021).
- [19] Xiang Lisa Li and Percy Liang. 2021. Prefix-tuning: Optimizing continuous prompts for generation. *arXiv preprint arXiv:2101.00190* (2021).
- [20] Ruixuan Liu, Tianhao Wang, Yang Cao, and Li Xiong. 2024. Precurious: How innocent pre-trained language models turn into privacy traps. In *Proceedings of the 2024 on ACM SIGSAC Conference on Computer and Communications Security*. 3511–3524.
- [21] Xiao-Yang Liu, Rongyi Zhu, Daochen Zha, Jiechao Gao, Shan Zhong, Matt White, and Meikang Qiu. 2025. Differentially private low-rank adaptation of large language model using federated learning. *ACM Transactions on Management Information Systems* 16, 2 (2025), 1–24.
- [22] Olivia Ma, Jonathan Passerat-Palmbach, and Dmitrii Usynin. 2024. Efficient and Private: Memorisation under differentially private parameter-efficient fine-tuning in language models. *arXiv preprint arXiv:2411.15831* (2024).
- [23] Saber Malekmohammadi and Golnoosh Farnadi. 2024. Low-Rank Adaptation Secretly Imitates Differentially Private SGD. *arXiv preprint arXiv:2409.17538* (2024).
- [24] Mitch Marcus, Beatrice Santorini, and Mary Ann Marcinkiewicz. 1993. Building a large annotated corpus of English: The Penn Treebank. *Computational linguistics* 19, 2 (1993), 313–330.
- [25] Ilya Mironov. 2017. Rényi differential privacy. In *2017 IEEE 30th computer security foundations symposium (CSF)*. IEEE, 263–275.
- [26] Alexander Novikov, Dmitrii Podoprikhin, Anton Osokin, and Dmitry P Vetrov. 2015. Tensorizing neural networks. *Advances in neural information processing systems* 28 (2015).
- [27] Ivan V Oseledets. 2011. Tensor-train decomposition. *SIAM Journal on Scientific Computing* 33, 5 (2011), 2295–2317.
- [28] Delong Ran, Xinlei He, Tianshuo Cong, Anyu Wang, Qi Li, and Xiaoyun Wang. 2025. Lora-leak: Membership inference attacks against lora fine-tuned language models. *arXiv preprint arXiv:2507.18302* (2025).
- [29] Noam Razin, Asaf Maman, and Nadav Cohen. 2021. Implicit regularization in tensor factorization. In *International Conference on Machine Learning*. PMLR, 8913–8924.
- [30] Reza Shokri, Marco Stronati, Congzheng Song, and Vitaly Shmatikov. 2017. Membership inference attacks against machine learning models. In *2017 IEEE symposium on security and privacy (SP)*. IEEE, 3–18.
- [31] Youbang Sun, Zitao Li, Yaliang Li, and Bolin Ding. 2024. Improving lora in privacy-preserving federated learning. *arXiv preprint arXiv:2403.12313* (2024).
- [32] Yuxin Wen, Lee Marchyok, Sanghyun Hong, Jonas Geiping, Tom Goldstein, and Nicholas Carlini. 2024. Privacy Backdoors: Enhancing Membership Inference through Poisoning Pre-trained Models. In *Advances in Neural Information Processing Systems (NeurIPS)*.
- [33] Jie Xu, Karthikeyan Saravanan, Rogier van Dalem, Haaris Mehmood, David Tuckey, and Mete Ozay. 2024. Dp-dylora: Fine-tuning transformer-based models on-device under differentially private federated learning using dynamic low-rank adaptation. *arXiv preprint arXiv:2405.06368* (2024).
- [34] Yifan Yang, Jiajun Zhou, Ngai Wong, and Zheng Zhang. 2024. LoRETTA: Low-Rank Economic Tensor-Train Adaptation for Ultra-Low-Parameter Fine-Tuning of Large Language Models. In *Proceedings of NAACL 2024*.
- [35] Samuel Yeom, Irene Giacomelli, Matt Fredrikson, and Somesh Jha. 2018. Privacy risk in machine learning: Analyzing the connection to overfitting. In *2018 IEEE 31st computer security foundations symposium (CSF)*. IEEE, 268–282.
- [36] Da Yu, Saurabh Naik, Arturs Backurs, Sivakanth Gopi, Huseyin A Inan, Gautam Kamath, Janardhan Kulkarni, Yin Tat Lee, Andre Manoel, Lukas Wutschitz, et al. 2021. Differentially private fine-tuning of language models. *arXiv preprint arXiv:2110.06500* (2021).

[37] Sajjad Zarifzadeh, Philippe Liu, and Reza Shokri. 2023. Low-cost high-power membership inference attacks. *arXiv preprint arXiv:2312.03262* (2023).

A Appendix A: Rank-wise Results and Extended Tables

This appendix reports additional results that are omitted from the main paper due to space constraints. In the main paper, we primarily present *rank-averaged* metrics to reduce sensitivity to any single adapter rank choice and to provide a robust comparison between LoRA and TTLoRA under differential privacy (DP). Here, we provide the *full rank-wise breakdown* for (i) validation perplexity (PPL) across privacy budgets and (ii) membership inference attack (MIA) metrics for each rank and ϵ .

How to read the tables. Across all appendix tables, lower ↓ is better for utility PPL and for attack metrics (AUC and FPR variants). Orange/blue highlights denote the best *individual* configuration within LoRA/TTLoRA respectively, while bold black indicates the best *average* between LoRA and TTLoRA (when an average row is present). Gray shading marks approximately parameter-matched configurations (to support controlled comparisons under comparable trainable parameter counts).

Non-private rank-wise reference on PTB. Finally, Table 5 provides non-private results on PTB across ranks. This table serves as a reference to interpret rank effects without DP noise and clipping. It also contextualizes the parameter–utility tradeoff across ranks: while larger ranks may yield diminishing improvements in PPL, they substantially increase trainable parameter counts, motivating the paper’s focus on the parameter-efficient regime and the use of rank-averaged reporting in the main sections.

Rank-wise DP perplexity trends. Table 6 reports validation PPL for all even ranks $r \in \{2, 4, \dots, 16\}$ across privacy budgets for Enron and PTB. These rank-wise results complement the rank-averaged trends in the main paper by showing that (1) PPL changes across ranks are typically modest within a fixed DP budget, and (2) the ordering across privacy budgets is consistent with the expected privacy–utility behavior (tighter privacy budgets generally yield higher PPL). This table also supports the interpretation that reporting rank-averaged PPL in the main paper is representative of the overall trend rather than dominated by a single rank.

Rank-wise DP attack trends on Enron and PTB. Tables 7 and 8 report rank-wise MIA results under DP for Enron and PTB respectively. For each ϵ , we report the attack AUC, FPR@10%, and utility PPL. These tables make two points explicit: (i) attack success generally increases as privacy becomes weaker (larger ϵ), consistent with standard DP expectations; and (ii) TTLoRA exhibits systematically reduced attack success compared to LoRA on average, while maintaining comparable utility, aligning with the privacy–utility trends reported in the main paper.

Table 5: Comparison of attack metrics (AUC, FPR@1%, FPR@0.01%) and utility (PPL) for LoRA, TTLoRA, and FFT on the PTB dataset.

Method	Rank	Params	PPL	AUC	FPR@1%	FPR@0.01%
LoRA	2	110.6k	25.95	98.55%	33.33%	0.57%
	4	221.2k	25.67	98.87%	44.54%	0.57%
	6	331.8k	25.46	98.81%	24.43%	0.57%
	8	442.4k	25.45	98.78%	23.56%	0.57%
	10	553.0k	25.42	98.87%	27.30%	0.57%
	12	663.6k	25.32	98.93%	28.45%	0.57%
	14	774.1k	25.29	99.00%	39.08%	0.57%
	16	884.7k	25.34	98.97%	39.37%	0.57%
	Avg.	497.7k	25.49	98.85%	32.51%	0.57%
TTLoRA	2	7.6k	27.81	89.81%	22.13%	1.15%
	4	18.2k	27.12	96.35%	39.66%	0.57%
	6	31.8k	26.69	97.80%	22.99%	0.57%
	8	48.4k	26.49	98.60%	34.20%	0.57%
	10	67.9k	26.38	98.74%	54.60%	0.86%
	12	90.4k	26.39	98.61%	27.01%	0.57%
	14	115.9k	26.26	98.69%	14.08%	0.57%
	16	144.4k	26.14	98.73%	22.70%	0.57%
	Avg.	65.6k	26.66	97.17%	29.67%	0.68%
FFT	–	124.04M	23.15	99.15%	64.94%	0.86%

Table 6: Comparison of Perplexity (Lower ↓ the better) on Enron and PTB datasets across different privacy budgets (ϵ) for different ranks.

Method	Params	Enron (ϵ)					PTB (ϵ)				
		0.5↓	1.0↓	3.0↓	5.0↓	Non-Priv.↓	0.5↓	1.0↓	3.0↓	5.0↓	Non-Priv.↓
LoRA											
Rank 2	110.59K	27.95	26.88	25.65	25.27	19.40	59.13	56.04	51.60	49.74	29.92
Rank 4	221.18K	28.38	27.11	25.98	25.64	18.95	59.54	57.14	53.19	51.70	29.22
Rank 6	331.78K	28.79	27.41	26.28	25.95	18.78	60.36	58.25	54.26	52.90	28.84
Rank 8	442.37K	29.05	27.68	26.58	26.25	18.73	60.32	58.68	54.89	53.56	28.64
Rank 10	552.96K	29.46	27.86	26.66	26.34	18.65	60.59	59.18	55.33	53.97	28.60
Rank 12	663.55K	29.89	28.09	26.81	26.47	18.63	60.65	59.62	55.84	54.42	28.61
Rank 14	774.14K	29.97	28.30	26.95	26.61	18.58	60.62	59.72	56.26	54.93	28.53
Rank 16	884.74K	30.84	28.51	28.18	27.96	18.58	60.76	60.10	56.64	55.19	28.51
Avg.	497.7K	29.29	27.62	26.64	26.44	18.79	60.41	58.59	54.75	53.81	28.86
TTLoRA											
Rank 2	7.63K	27.71	26.51	24.69	24.34	22.25	57.56	54.03	49.66	48.25	37.32
Rank 4	18.24K	27.28	25.92	24.65	24.40	21.08	58.25	54.71	49.59	47.59	33.58
Rank 6	31.82K	27.62	26.52	24.92	24.51	20.42	57.60	54.89	50.35	48.45	32.04
Rank 8	48.38K	27.63	26.90	25.57	25.11	19.97	58.05	55.77	51.82	50.03	30.84
Rank 10	67.92K	27.29	26.44	25.20	24.75	19.65	58.58	55.47	50.01	48.00	30.09
Rank 12	90.43K	27.47	26.74	25.92	25.45	19.40	58.92	55.91	50.54	48.47	29.58
Rank 14	115.92K	27.44	26.67	25.94	25.58	19.17	58.77	55.60	50.96	48.96	29.25
Rank 16	144.38K	27.84	27.04	26.27	25.93	19.02	60.02	56.77	51.96	49.91	28.91
Avg.	65.6K	27.52	26.55	25.37	24.99	20.14	58.47	55.39	50.61	48.71	31.45
FFT	124.04M	28.81	27.05	25.38	24.92	14.31	56.18	53.38	49.23	47.79	19.75

Table 7: Comparison of Attack Metrics (AUC and FPR@10%) and utility (PPL) for LoRA and TTLoRA across Enron dataset for ϵ values. Lower ↓ is better for AUC, FPR@10%, and PPL.

Method	Epsilon (ϵ)											
	0.5			1.0			3.0			5.0		
	AUC	PPL	FPR@10%	AUC	PPL	FPR@10%	AUC	PPL	FPR@10%	AUC	PPL	FPR@10%
LoRA												
Rank2	54.79%	20.72	11.69%	56.91%	20.72	12.89%	61.14%	20.71	17.24%	62.32%	20.70	19.49%
Rank4	54.33%	20.72	12.59%	56.44%	20.72	14.69%	60.57%	20.71	17.00%	61.99%	20.70	18.14%
Rank6	52.25%	20.72	12.74%	54.11%	20.72	13.19%	57.86%	20.71	17.84%	59.36%	20.71	16.34%
Rank8	50.06%	20.72	9.90%	50.79%	20.72	10.49%	52.76%	20.72	11.99%	53.94%	20.72	11.69%
Rank10	51.14%	20.72	10.04%	53.08%	20.72	11.69%	57.30%	20.71	15.89%	58.94%	20.71	16.79%
Rank12	51.91%	20.71	11.00%	50.72%	20.71	10.94%	52.67%	20.71	11.84%	54.44%	20.71	13.34%
Rank14	53.27%	20.71	11.39%	54.71%	20.71	12.89%	58.25%	20.71	13.49%	59.74%	20.71	16.64%
Rank16	52.15%	20.72	9.75%	52.99%	20.72	10.04%	55.36%	20.72	13.94%	56.72%	20.72	14.69%
Avg.	52.49%	20.72	11.14%	53.72%	20.72	12.10%	56.99%	20.71	14.90%	58.43%	20.71	15.89%
TTLoRA												
Rank2	52.87%	20.78	12.44%	53.65%	20.75	13.19%	55.54%	20.73	14.39%	56.46%	20.72	14.54%
Rank4	52.37%	20.73	9.45%	52.12%	20.72	9.15%	51.27%	20.72	9.00%	50.84%	20.72	9.00%
Rank6	50.75%	20.72	10.64%	51.05%	20.72	10.94%	51.79%	20.72	11.39%	52.19%	20.72	11.09%
Rank8	50.77%	20.71	9.00%	51.13%	20.71	9.00%	51.88%	20.71	9.90%	52.47%	20.71	10.04%
Rank10	50.74%	20.72	13.49%	50.94%	20.72	13.64%	51.27%	20.72	12.74%	51.51%	20.72	13.04%
Rank12	51.10%	20.72	11.54%	50.67%	20.72	12.44%	50.23%	20.72	13.19%	50.63%	20.72	13.49%
Rank14	50.39%	20.72	8.40%	50.27%	20.72	8.25%	50.06%	20.72	8.10%	50.07%	20.72	7.80%
Rank16	51.91%	20.72	10.34%	51.97%	20.72	10.34%	52.05%	20.72	10.79%	52.10%	20.72	10.79%
Avg.	51.36%	20.72	10.66%	51.48%	20.72	10.87%	51.76%	20.72	11.19%	52.03%	20.72	11.22%
FFT	54.38%	20.96	13.04%	55.22%	20.88	13.04%	56.85%	20.76	13.34%	57.72%	20.72	13.49%

Table 8: Comparison of Attack Metrics (AUC and FPR@10%) and utility (PPL) for LoRA and TTLoRA across PTB dataset for ϵ values. Lower \downarrow is better for AUC, FPR@10%, and PPL.

Method	Epsilon (ϵ)											
	0.5			1.0			3.0			5.0		
	AUC%	PPL	FPR@10%	AUC%	PPL	FPR@10%	AUC%	PPL	FPR@10%	AUC%	PPL	FPR@10%
LoRA												
Rank2	53.90%	32.32	11.21%	55.02%	31.91	12.07%	58.41%	31.42	16.67%	60.18%	31.25	18.39%
Rank4	51.35%	32.31	7.76%	52.69%	31.90	10.06%	56.75%	31.40	11.49%	58.88%	31.23	16.38%
Rank6	52.14%	32.35	13.22%	53.53%	31.94	15.23%	57.47%	31.43	19.83%	59.78%	31.27	21.26%
Rank8	52.89%	32.34	10.92%	51.96%	31.93	12.07%	50.77%	31.42	11.49%	52.66%	31.26	13.51%
Rank10	53.02%	32.36	12.93%	54.22%	31.95	15.23%	57.70%	31.45	19.25%	59.70%	31.29	22.41%
Rank12	52.30%	32.32	8.91%	53.37%	31.91	9.77%	56.29%	31.41	12.36%	58.13%	31.25	15.80%
Rank14	53.88%	32.38	13.51%	55.17%	31.97	13.79%	58.96%	31.46	18.68%	61.16%	31.31	21.84%
Rank16	51.49%	32.34	8.62%	52.61%	31.93	9.20%	56.06%	31.43	12.36%	58.11%	31.26	15.52%
Avg.	52.62%	32.34	10.88%	53.57%	31.93	12.18%	56.55%	31.43	15.27%	58.58%	31.27	18.14%
TTLoRA												
Rank2	52.00%	32.31	8.91%	51.55%	31.91	8.62%	50.03%	31.41	6.90%	51.05%	31.25	6.90%
Rank4	52.52%	32.32	8.05%	52.97%	31.91	7.18%	53.55%	31.42	8.62%	53.87%	31.25	10.63%
Rank6	52.98%	32.32	6.03%	52.91%	31.92	6.32%	52.70%	31.43	7.76%	52.49%	31.26	6.61%
Rank8	50.83%	32.35	12.07%	51.05%	31.94	11.78%	51.75%	31.45	11.21%	52.17%	31.28	10.34%
Rank10	50.90%	32.36	12.07%	50.81%	31.96	12.07%	50.67%	31.46	12.36%	50.58%	31.30	12.93%
Rank12	52.03%	32.35	9.48%	52.31%	31.95	9.77%	53.24%	31.45	9.48%	53.89%	31.28	10.92%
Rank14	51.46%	32.35	8.62%	51.58%	31.95	8.62%	51.96%	31.44	8.05%	52.26%	31.28	8.05%
Rank16	50.25%	32.38	10.06%	50.02%	31.98	10.34%	50.66%	31.48	11.21%	51.18%	31.31	12.36%
Avg.	51.62%	32.34	9.41%	51.65%	31.94	9.34%	51.82%	31.44	9.45%	52.19%	31.28	9.84%
FFT	51.21%	31.74	8.33%	50.94%	31.70	8.33%	50.69%	31.61	13.79%	52.23%	31.57	14.37%